Influence of Hot Electron Scattering and Electron–Phonon Interactions on Thermal Boundary Conductance at Metal/Nonmetal Interfaces

Ashutosh Giri
Department of Mechanical and Aerospace Engineering, University of Virginia, Charlottesville, VA 22904
e-mail: ag4ar@virginia.edu

Brian M. Foley
Department of Mechanical and Aerospace Engineering, University of Virginia, Charlottesville, VA 22904
e-mail: bmf4su@virginia.edu

Patrick E. Hopkins
Department of Mechanical and Aerospace Engineering, University of Virginia, Charlottesville, VA 22904
e-mail: phopkins@virginia.edu

It has recently been demonstrated that under certain conditions of electron nonequilibrium, electron to substrate energy coupling could represent a unique mechanism to enhance heat flow across interfaces. In this work, we present a coupled thermodynamic and quantum mechanical derivation of electron–phonon scattering at free electron metal/nonmetal substrate interfaces. A simplified approach to the Fermi's Golden Rule with electron energy transitions between only three energy levels is adopted to derive an electron–phonon diffuse mismatch model, that account for the electron–phonon thermal boundary conductance at metal/insulator interfaces increases with electron temperature. Our approach demonstrates that the metal-electron/nonmetal phonon conductance at interfaces can be an order of magnitude larger than purely phonon driven processes when the electrons are driven out of equilibrium with the phonons, consistent with recent experimental observations. [DOI: 10.1115/1.4027785]

Keywords: nonequilibrium electron transport, electron–phonon coupling, diffuse mismatch model, two-temperature model, thermal boundary conductance, metal–nonmetal interfaces

1 Introduction

The underlying physics driving thermal transport and scattering at the submicron length scale has been an active area of research over the past few decades [1–3]. One of the main challenges has been to characterize the role of the interface between nanostructures on the energy transport processes. Kapitza [4] quantified the thermal boundary conductance, h_K, as the ratio of the heat flux across the interfacial region to the temperature drop ΔT. Since the scattering mechanisms of the fundamental energy carriers (i.e., electrons and phonons) at the interface influence the h_K [5], advancing the theoretical understanding of these scattering processes is of utmost importance to advancing nanotechnology.

Electrons are the primary heat carriers in metals and phonons dominate the transport process in insulators and semiconductors. Therefore, the heat transport pathway between two metals is dominated by the scattering of electrons that transport energy through the interface [6–9]. However, at a metal/nonmetal interface, the electrons cannot physically transmit to the nonmetal (assuming large barrier heights and no tunneling), and previous theories and experiments have alluded to various electron and/or phonon scattering processes that drive this transport pathway [1,3,5,10,11].

Stoner and Maris [12,13] reported on the measurements of h_K between a series of metals and dielectrics. They compared their experimental findings to various phonon–phonon scattering models [14] and found discrepancies for interfaces with soft metals (Ag and Pb). Their findings led Huberman and Overhauser [15] and Sergeev [16,17] to propose a different channel for energy conduction. Their works were rooted in theories of conventional electron–phonon scattering, such as the deformation potential interaction [18]. More recently, Mahan [19] presented a theory on electron-metal/phonon-nonmetal interactions that involves the image potential theory. Regardless of the theoretical mechanism, all of these aforementioned works [15,16,19] point to the fact that the measurements of thermal boundary conductance between metals and nonmetals in Stoner and Maris' [12,13] works were driven by metal electrons directly interacting with the nonmetal phonons.

Since Stoner and Maris' seminal works [12,13], Lyeo and Cahill [20] have shown that electron-interface scattering does not significantly contribute to the thermal boundary conductance at metal/nonmetal interfaces. Their results show that this interfacial conductance is driven by phonon scattering, as Pb and Bi, which have similar Debye temperatures yet different electron densities around their respective Fermi surfaces, have similar rates of thermal boundary conductance across the diamond interfaces. We have also confirmed Lyeo and Cahill's experimental findings with various phonon–phonon scattering theories [21–23]. In addition, a recent work by Singh et al. [24] has shown that at noncryogenic temperatures, electron-metal/phonon-nonmetal scattering does not contribute to thermal processes. In light of these recent works, the transport across a metal/nonmetal interface is most likely primarily driven by phonon–phonon interactions in the regime of moderate electron and lattice temperatures and assuming the electrons and lattice are defined by relatively similar temperatures (i.e., $T_e - T_0 \ll T_0$, where T_e is the electron temperature and T_0 is the lattice temperature). This supports the electron–phonon interfacial mechanism proposed by Majumdar and Reddy [25] in which electron–phonon coupling in the bulk of the metal must occur before phonon–phonon scattering transmits energy across a metal/nonmetal interface.

To the previous paragraphs' discussions and statements, we have experimentally shown that electron-interface scattering can change the overall rate of electron–phonon equilibration of a thin Au film when the electrons have a different energy density than the lattice [26,27]. Guo et al. [28] have also shown the interface

Contributed by the Heat Transfer Division of ASME for publication in the Journal of Heat Transfer. Manuscript received November 4, 2013; final manuscript received May 22, 2014; published online June 12, 2014. Assoc. Editor: Ali Khounsary.

dependency of the electron–phonon coupling factor, G. These works speculated that when the film thickness is less than the electron–phonon mean free path, electron-interface scattering can result in an increase in electron–phonon coupling [26–28]. An additional finding from these works determined that as the degree of electron–phonon nonequilibrium increases (i.e., as the electron temperature increases and $T_e - T_0 \gg T_0$), the electron-interface scattering mechanism increases. This suggests an additional channel for thermal transport across interfaces that are solely driven by the scattering of metal electrons on the interface and exchanging energy to the nonmetal substrate. Previous theories on electron–phonon scattering cannot account for this electronic scattering mechanism and resulting enhancement in thermal boundary conductance: [15,16,19,24,29] The key to capturing this phenomenon is that the electrons in the metal are highly out of equilibrium with the phonons in the metal and substrate.

In this paper, we develop the theory of electron–phonon interactions at metal/nonmetal interfaces, and the resulting thermal boundary conductance, h_K, in the case when the electrons in the metal are defined by a different temperature than the metal and substrate lattices. We show acceptable agreement with our previous experimental measurements, lending insight into the fundamental mechanisms that drive this large pathway for heat conduction across interfaces. The theory presented in this work is consistent with previous seminal works that derived analytical expressions for G in metals [30,31]. Kaganov et al. [31] derived the rate of electron–phonon energy exchange in a free electron metal based off of the thermal population of the interacting phonon system and the probability of electron energy transitions [31]. Qiu and Tien later rederived the electron–phonon coupling factor in free electron metals by considering the interacting electron number density at the phonon emission or absorption energy during electron–phonon scattering events [30]. Using the approaches described in both these seminal works, we derive the metal/nonmetal thermal boundary conductance based on the probability of electron transitions in a metal driven by emission or absorption of substrate phonons.

2 Electron Energy Exchange at a Metal/Nonmetal Interface

Due to their femtosecond resolution, short-pulsed lasers have been widely used to understand the scattering mechanisms of the fundamental energy carriers. To quantitatively predict these highly nonequilibrium processes in metals, theoretical and computational studies have employed the two-temperature model [32] that describes the temporal and spatial evolution of the electronic and lattice temperatures during ultrafast laser heating. The absorption of the laser pulse by the metal surface and the subsequent energy relaxation processes thereafter can be described by three characteristic time intervals: (i) the thermalization of the free electron gas, (ii) the coupling between electrons and the lattice; and (iii) the energy transport driven by the gradient in the lattice temperature [33].

The metal electrons are defined by a range of energies resulting from the equivalent equilibrium temperature of the thermalized electrons and degree of Fermi smearing. In a free electron metal, the vast majority of excited electrons that are losing energy to the lattice are on the Fermi surface with energies of some $\delta\varepsilon$ around the Fermi energy. For free electron metals with a relatively constant density of states (DOS) around the Fermi energy, $\delta\varepsilon = \hbar\omega \ll \Delta\varepsilon_F$, where ε_F is the Fermi energy and $\Delta\varepsilon_F$ is the width of the constant energy DOS around the Fermi energy (for example, assuming gold electrons interacting with silicon substrate phonons, the maximum phonon energy available for metal-electron energy interaction is $\hbar\omega \approx h(15\text{THz}) \approx 0.06\,\text{eV}$ which is much less than the Fermi level to $5d^{10}$-band edge energy separation in gold, $\Delta\varepsilon_F \approx 1.8\,\text{eV}$) [34]. Therefore, the electron energy and population interacting with the phonons in a free electron noble metal will not deviate from those at the Fermi energy as the energy states of electrons before and after the collisions are very close.

For the calculations in this work, we assume a constant lattice temperature of $T_0 = 296\,\text{K}$ due to the high thermal effusivities of the substrates under study (Si, Ge, diamond). In other words, even the maximum absorbed laser fluence considered in this work will only raise the temperature of the substrate lattice by a couple of degrees which has negligible influence on the calculated electron-substrate thermal boundary conductance. It should also be noted that the thermalization time of the electrons could be in the order of the electron–phonon relaxation time depending on the absorbed laser fluence [35,36], therefore, we use an effective electron temperature ($T_{e,\text{eff}}$) to describe the electron system hereafter. Assuming an isotropic metal, the electron-substrate energy transfer across the interface is given by

$$h_{es} = \frac{1}{4}\int_{\varepsilon} (\varepsilon - \varepsilon_F) D_e(\varepsilon) \frac{\partial f}{\partial T_{e,\text{eff}}} v_f \xi_{\text{int}} d\varepsilon \tag{1}$$

where ε is the electron energy, D_e is the DOS for electrons, v_f is the Fermi velocity, f is the electron distribution function, and ξ_{int} is the transmission coefficient. The critical parameter in calculating the thermal boundary conductance is the transmission coefficient.

Electron–phonon scattering processes involve the redistribution of electrons among the allowed energy states by either emitting or absorbing phonons. During this process, electrons can be forced into or out of an energy state. Assuming single phonon emission or absorption from electron–phonon collisions [30], the energy of the electrons and the subsequent phonons can be well defined. The transition probabilities from an electron distribution f to a different distribution f' by emitting a phonon is proportional to $f(1-f')(N+1)$, where N describes the Bose–Einstein distribution of phonons with a particular vibrational frequency. The $N+1$ term represents the phonon emission probability that includes both the stimulated and spontaneous emission. Similarly, the transition probability that involves absorption of a phonon by an electron distribution f to a distribution f' is proportional to $f(1-f')(N)$. The total rate of change of electron density in a particular distribution f can most rigorously be derived with Fermi's Golden Rule and the electron–phonon interaction matrix over all energy states [18]. However, Qiu and Tien [30] offered a simple three-level electronic transition picture to calculate the electron–phonon interaction probability based on the electron and phonon distributions at different energies. This approach agreed with Kaganov et al.'s [31] approach and is therefore adopted in this work.

Following Qiu and Tien [30], we assume that electronic transitions take place between three energy levels: $\varepsilon_F - \hbar\omega, \varepsilon_F$, and $\varepsilon_F + \hbar\omega$. Considering that $\delta\varepsilon \ll \varepsilon_F$, these are reasonable assumptions. With these transitions, we can then define the total electronic transition probability as the sum of each individual transition probability in our simple three-level system [30] given by

$$\begin{aligned}\xi_{\text{int}}(\omega) = {} & \eta_{\varepsilon_F - \hbar\omega \to \varepsilon_F}(\omega) + \eta_{\varepsilon_F + \hbar\omega \to \varepsilon_F}(\omega) + \eta_{\varepsilon_F \to \varepsilon_F - \hbar\omega}(\omega) \\ & + \eta_{\varepsilon_F \to \varepsilon_F + \hbar\omega}(\omega)\end{aligned} \tag{2}$$

where $\eta_{\varepsilon_F - \hbar\omega \to \varepsilon_F}$ is the probability of an electronic transition from the $\varepsilon_F - \hbar\omega$ energy level to the Fermi energy, ε_F. The other probabilities are defined similarly based on the subscripts of η. This is shown schematically in Fig. 1.

Phonon absorption in the metal causes an electronic transition from a lower to a higher energy level, where phonon emission from the metal causes an electronic transition from a higher to a lower energy level. These electronic transition probabilities (η_A for phonon absorption and η_E for phonon emission) are related to the occupancy of the electronic energy levels. Therefore, the transition probability from energy $\varepsilon_F + \hbar\omega$ to ε_F by emitting a phonon is

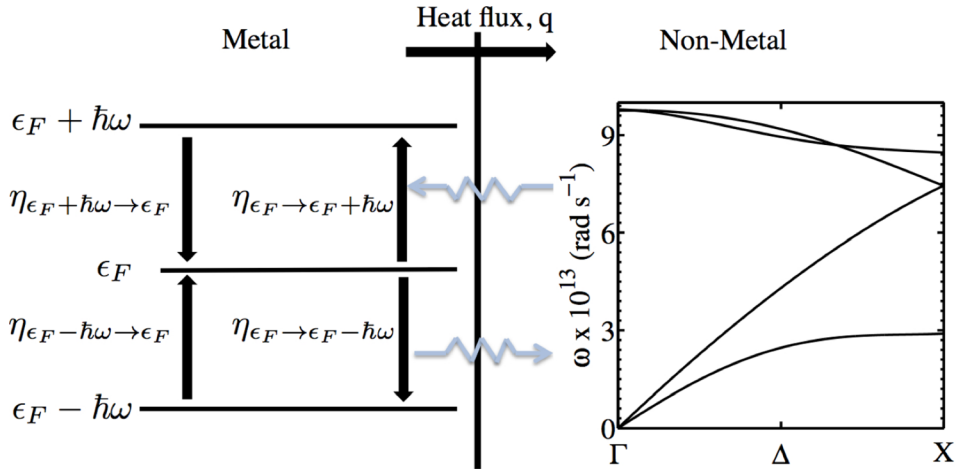

Fig. 1 Schematic diagram showing the transitions in the three energy levels in the metal and phonon frequencies in the nonmetal that we account for in this work. For our calculation of h_{es} of Au/Silicon in this paper, we use the phonon dispersion relation for silicon along the $\Gamma \to X$ direction computed by Weber [37].

$$\eta_{\varepsilon_F+\hbar\omega\to\varepsilon_F}(\omega) = f(\varepsilon_F+\hbar\omega)[1-f(\varepsilon_F)]\zeta_E = \frac{\zeta_E}{2\left(1+\exp\left(\frac{\hbar\omega}{k_B T_{e,eff}}\right)\right)} \tag{3}$$

where ζ_E is the probability of emitting a phonon [30]. Similarly

$$\eta_{\varepsilon_F-\hbar\omega\to\varepsilon_F}(\omega) = f(\varepsilon_F-\hbar\omega)[1-f(\varepsilon_F)]\zeta_A = \frac{\zeta_A}{2\left(1+\exp\left(-\frac{\hbar\omega}{k_B T_{e,eff}}\right)\right)} \tag{4}$$

where ζ_A is the probability of absorbing a phonon. Note that $\eta_{\varepsilon-\hbar\omega\to\varepsilon_F} = \eta_{\varepsilon_F\to\varepsilon_F+\hbar\omega}$ and $\eta_{\varepsilon+\hbar\omega\to\varepsilon_F} = \eta_{\varepsilon_F\to\varepsilon_F-\hbar\omega}$ for the same phonon frequency, ω.

In a homogeneous material, the probability of absorption or emission of a phonon from electron–phonon collisions is given by [30]

$$\zeta_A = \frac{1}{\exp\left(\frac{\hbar\omega}{k_B T_0}+1\right)} \tag{5}$$

and

$$\zeta_E = \frac{\exp\frac{\hbar\omega}{k_B T_0}}{\exp\left(\frac{\hbar\omega}{k_B T_0}+1\right)} \tag{6}$$

respectively, where $\zeta_A \equiv 1-\zeta_E$ for a homogeneous material when $T_{e,eff} = T_0$. At an interface between a metal and nonmetal, these probabilities are different. Therefore, ζ_A and ζ_E must be redefined for the interface problem. In other words, we must determine the probability of electron energy transitions in the metal due to phonon emission or absorption with the nonmetal.

The transmission probability of heat fluxes at solid interfaces has been addressed specifically for electron–electron [8,38] and phonon–phonon [10] interactions for noncryogenic temperature regimes by considering diffusive scattering of energy carriers (i.e., the diffuse mismatch model approach) [10]. In this approach, the carriers are assumed to scatter diffusively and the transmission probability is determined by equating the thermal fluxes on either side of the interface via the principle of detailed balance (in-depth treatments regarding these assumptions are discussed in Refs. [39,40], respectively). In short, our fundamental assumption of diffuse scattering implies that incident carriers lose all memory of their initial direction after scattering at the interface. For each ω, we equate the heat fluxes on either side given by

$$\begin{aligned}\hbar\omega(D_{p,L}(k_L)+2D_{p,T}(k_T))v_f f(\varepsilon_F-\hbar\omega,T_{e,eff})\zeta_{m,E} &= \hbar\omega(N(\hbar\omega,T_0)+1)(D_{p,L}(k_L)v_{g,L} \\ &+ 2D_{p,T}(k_T)v_{g,T})\zeta_{nm,A}\end{aligned} \tag{7}$$

which relates the phonon emission via metal-electron relaxation to phonon absorption in the nonmetal and

$$\begin{aligned}\hbar\omega(D_{p,L}(k_L)+2D_{p,T}(k_T))v_f f(\varepsilon_F+\hbar\omega,T_{e,eff})\zeta_{m,A} &= \hbar\omega N(\hbar\omega,T_0)(D_{p,L}(k_L)v_{g,L} \\ &+ 2D_{p,T}(k_T)v_{g,T})\zeta_{nm,E}\end{aligned} \tag{8}$$

which relates the phonon absorption via metal-electron excitation to phonon emission in the nonmetal. In these expressions, $D_{p,L}$ and $D_{p,T}$ are the densities of states for longitudinal and transverse mode phonons in the nonmetal, respectively, k_L and k_T are the wave-vectors for the corresponding longitudinal and transverse phonon frequencies, respectively, $v_{g,L}$ and $v_{g,T}$ are the longitudinal and transverse phonon group velocities, respectively, and N is the Bose–Einstein distribution function. The $\zeta_{(m,E),(nm,A),(m,A),(nm,E)}$ terms are the probability of emission (E) and absorption (A) by metal (m) and nonmetal (nm). The $D_{p,j}$ terms appear on the flux from the metal side due to our assumption of single phonon absorption or emission during the collision process; in other words, the number of quantum states and energy of electrons in the metal interacting with the nonmetal must be equal to the number of quantum states and energy of phonons in the nonmetal. The phonon DOS in the nonmetal is given by

$$D_{p,j}(k_j) = \frac{k_j^2}{2\pi^2 v_{g,j}} \tag{9}$$

where the index j represents the summation over all the polarizations of the phonons in the nonmetal. From the assumption of diffuse scattering, we have $1-\zeta_{m,E} = \zeta_{nm,A}$ and $1-\zeta_{m,A} = \zeta_{nm,E}$. Therefore, Eqs. (7) and (8) can be rearranged to determine the metal emission and absorption probabilities at phonon frequency, ω

$$\zeta_{m,E}(\omega, T_{e,eff}, T_0) = \frac{(N(\hbar\omega, T_0)+1)(k_L+2k_T)}{v_{tf}f(\varepsilon-\hbar\omega, T_{e,eff})\left(\frac{k_L}{v_{g,L}}+\frac{2k_T}{v_{g,T}}\right)+(N(\hbar\omega, T_0)+1)(k_L+2k_T)} \quad (10)$$

$$\zeta_{m,A}(\omega, T_{e,eff}, T_0) = \frac{N(\hbar\omega, T_0)(k_L+2k_T)}{v_{tf}f(\varepsilon+\hbar\omega, T_{e,eff})\left(\frac{k_L}{v_{g,L}}+\frac{2k_T}{v_{g,T}}\right)+N(\hbar\omega, T_0)(k_L+2k_T)} \quad (11)$$

In these expressions, we assume two degenerate transverse phonon branches.

3 Results

Using Eqs. (10) and (11) with Eqs. (3) and (4), the spectral transition probability of electrons due to nonmetal phonon interaction is determined via Eq. (2). We show calculations of η_A and η_E as a function of the phonon angular frequency, ω, for a gold film on a silicon substrate in Fig. 2(*a*). In our calculations, we consider the phonon dispersion relation for silicon along the $\Gamma \rightarrow X$ direction computed by Weber in Ref. [37]. This was previously demonstrated to be an acceptable assumption for calculating phonon properties of silicon [41]. The electronic transition probabilities show very strong frequency dependence for low frequency phonons in the nonmetal substrate (Fig. 2(*a*)). This can be attributed to the two transverse acoustic modes and one longitudinal acoustic vibrations taking part in the interfacial energy exchange in the Si substrate. At $\omega \sim 3 \times 10^{13}$ rads^{-1}, there is an abrupt drop in the transition probabilities due to the very low group velocities of the two transverse modes around this frequency threshold. For 300 K, effective electron temperature, the probability of phonon absorption is higher than phonon emission whereas at 3000 K, the scenario is reversed. To show this more quantitatively, we plot the average electronic transition probability (considering the full phonon dispersion of silicon) as a function of effective electron temperature, $T_{e,eff}$ (Fig. 2(*b*)). As expected, the average electronic transition probability for absorption, $\bar{\eta}_A$, decreases, while the $\bar{\eta}_E$ increases as the effective electron temperature increases. Replacing these probabilities in Eq. (2) gives the total electronic transition probability due to interface scattering and ultimately allows for the prediction of thermal boundary conductance between the electrons in a metal and the phonons in a nonmetal interface as a function of the metal-effective electron temperature (Eq. (1)). Figure 3 shows the theoretically calculated h_{es} for gold film on a silicon substrate. Our predicted values agree well with the experimental data from our previous work [27].

It is well known that at the onset of ultrashort laser pulse absorption on metal surfaces, the electrons relax to a Fermi distribution through various collisions while ballistically traversing through the metal film. However, in the scenario when the metal film thickness is less than the ballistic length scale of the electrons, the electrons will lose energy to the substrate, and the resulting thermal boundary conductance of this hot electron, substrate phonon transport mechanism across Au/silicon interfaces is well captured by our model. Based on the agreement of our theoretical model and experimental data, we can conclude that the temperature dependence in h_{es} arises due to the energy of the electrons in the metal (i.e., the temperature dependence of the electronic heat capacity); this is similar to the conclusion found for the electron thermal boundary conductance across metal/metal interfaces [8].

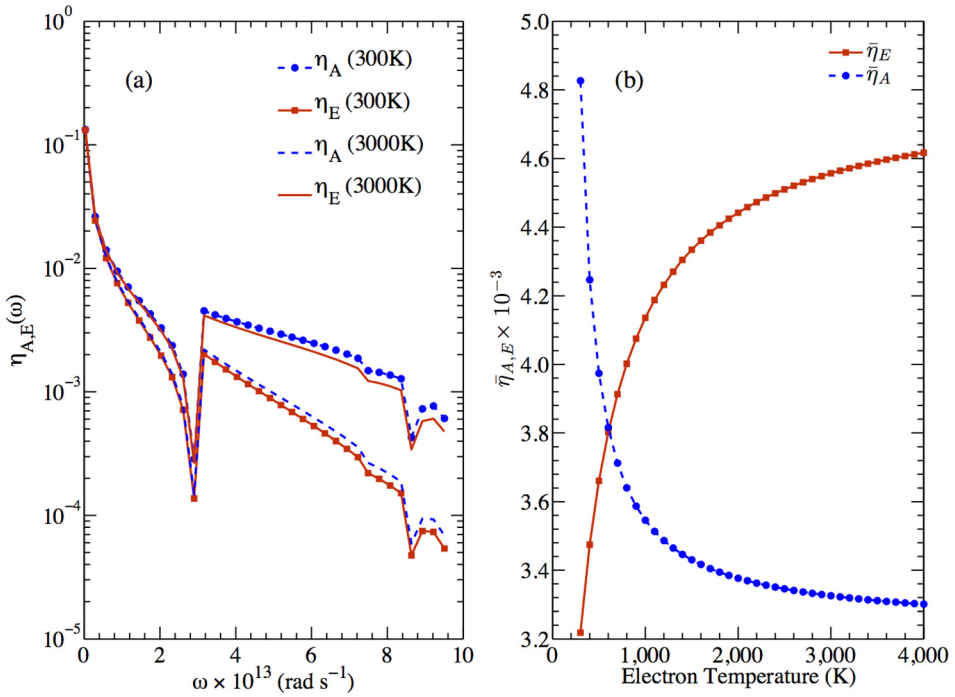

Fig. 2 (*a*) Electronic transition probabilities in a gold film as a function of the phonon angular frequency of Si at 300 K and 3000 K effective electron temperatures. The probability of absorbing a phonon is higher than the probability of emitting a phonon at 300 K but at 3000 K, the probability of emission is higher. There is a sharp drop in the probabilities at $\omega \approx 3\times10^{13}$ rads^{-1} due to the low group velocities of the transverse acoustic modes near the Brillouin zone edge. (*b*) Average electronic transition probability, $\bar{\eta}_{A,E}$, as a function of temperature. For low temperatures $T_{e,eff} \leq 800$ K, the average probability of absorbing phonons is higher than that for emitting phonons. As temperature increases, the phonon emission probability increases while the phonon absorption probability decreases.

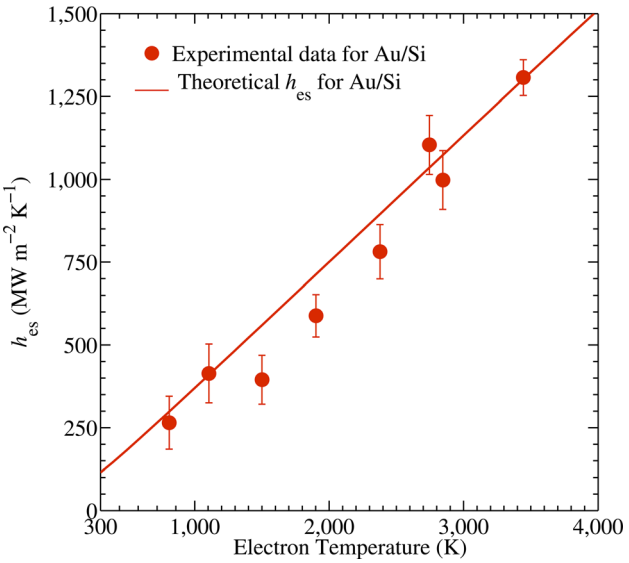

Fig. 3 h_{es} predicted from the theoretical framework developed in this work compared with the experimentally determined h_{es} from the thermoreflectance data analyzed with the two-temperature model [27]. The h_{es} increases linearly with increasing effective electron temperature.

To examine the influence of the phonon dispersion on the thermal boundary conductance, we repeat our calculations for Au/Ge and Au/diamond assuming the Ge and diamond dispersion from Ref. [37]. Figure 4 shows the comparison between the three systems for the electron-substrate thermal boundary conductance as a function of effective electron temperature. It is clear that by changing the phonon frequency spectrum of the nonmetal substrate, the electron-substrate energy transfer changes as well. At 296 K, the phonon DOS in Ge is relatively higher than that in Si and diamond. Electrons in the metal side have higher transition probabilities as the number of phonon states increases in the nonmetal side. This leads to an increase in the electron-substrate energy transfer across the interface in Au/Ge compared to Au/Si and Au/diamond.

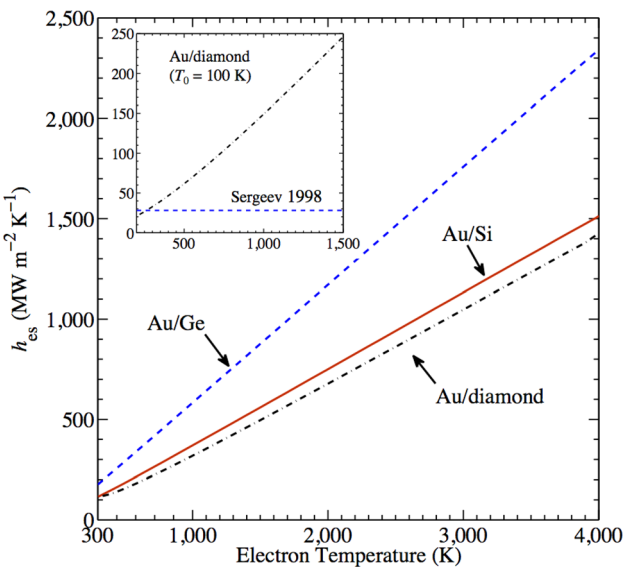

Fig. 4 h_{es} as a function of effective electron temperature for Au/Si (red solid line), Au/Ge (dashed line), and Au/diamond (dashed-dot line) at $T_0 = 300$ K, substrate temperature. The values of the predicted h_{es} are different for different phonon dispersions of the substrate. (Inset) For comparison, we have also plotted Kapitza conductance for Au/diamond at $T_0 = 100$ K as a function of electron temperature and the model prediction from Ref. [16] for negligible electron–phonon nonequilibrium.

In addition to the linear dependence of h_{es} on the effective electron temperature based on conservation of energy considerations, our model suggests that the majority of the electron–phonon interaction is driven by the low frequency phonons in the substrate (Fig. 2). This alludes to the fact that the assumption of electron interaction with phonons contributing to the second moment to the phonon spectrum [18] is valid even at interfaces between dissimilar materials. Moreover, as shown in the inset of Fig. 4, the predicted values of h_{es} for a Au/diamond interface at a lattice temperature of 100 K approach 20 MW m^{-2} K^{-1}, which is in acceptable agreement with separate theories for electron–phonon energy exchange across the interface [16,17]. As is clear, for the case of equilibrium between electrons in the metal and phonons in the substrate, our model predictions agree with the experimentally measured values of Kapitza conductance across metal/nonmetal interfaces, such as our recent experimental measurements of the phonon-dominated thermal boundary conductance between Au/Silicon [42]. However, the phonon-dominated thermal boundary conductance exhibits a different temperature trend than the hot electron, phonon substrate driven thermal boundary conductance shown in Figs. 3 and 4. Where the hot electron–phonon boundary conductance is driven by the electron energy (i.e., electron heat capacity temperature trends), the phonon–phonon driven thermal boundary conductance is driven by the lattice energy (i.e., phonon heat capacity temperature trends). Interestingly, the relative values are similar for equal electron and lattice temperatures, but these two transport mechanisms are inherently different, and the differentiation between the two can only be realized by examining the temperature trends, at least for Au/Si.

This begs an important question for future works: when is the electron–phonon interface interaction more probable than the phonon–phonon interface interaction? We did not address this specifically in our current work, as more rigorous analytical or computational theories are required to answer this question. However, our previous experimental works suggest that the h_{es} pathway is driven by ballistic electrons in a nonthermal distribution [27] and [43]. Although this is beyond the scope of our current theories, nonequilibrium statistical mechanisms coupled with transition probability theories could be used to theoretically investigate the interplay between electron–phonon and phonon–phonon interfacial interactions.

4 Summary

In summary, we have derived a theoretical model to predict the thermal boundary conductance across metal/nonmetal interfaces due to electron–phonon interactions. By performing calculations on a gold film on silicon substrate, we have shown that our theory agrees with our previous experimental findings. With analysis of our model calculations, we conclude that the electron–phonon thermal pathway across metal/nonmetal interfaces is driven by the electron energy density and an interplay between temperature dependent phonon emission and absorption probabilities. We caution that this effect has only been conclusively observed at Au/Si interfaces in which the Au electrons are out of equilibrium with the lattice. Future theoretical works should focus on the interplay between this electron–phonon and phonon–phonon energy transmission pathways across interfaces. This will yield a more holistic view of thermal boundary conductance across metal/nonmetal interfaces, and the role of both temporal and spatial scales on these processes.

Acknowledgment

P.E.H. recognizes support from the AFSOR Young Investigator Program (FA9550-13-1-0067). A.G. is grateful to Chris Baker at U.V.A for critical reading of the manuscript.

Nomenclature

D = DOS per volume
f = Fermi-Dirac distribution function for electrons
G = electron–phonon coupling factor (W m^{-3} K^{-1})
$\hbar$ = Plank's constant divided by 2π (J s)
h_K = thermal boundary conductance (W m^{-2} K^{-1})
k = phonon wavevector (rad m^{-1})
k_B = Boltzmann's constant (J K^{-1})
N = Bose–Einstein distribution function for phonons
T_e = electron temperature (K)
T_0 = lattice temperature (K)
v_f = Fermi velocity (m s^{-1})
v_g = phonon group velocity (m s^{-1})

Greek Symbols

Δ = change in
ε = electron energy, eV
ε_F = Fermi energy, eV
η = probability of emitting or absorbing a phonon
ξ = interfacial transmission coefficient
ω = angular frequency of vibration, rad s^{-1}

Subscript

A = absorption
e,eff = effective electron
E = emission
es = electron-substrate
int = interfacial
j = polarization
L = longitudinal mode
m = metal
nm = nonmetal
p = phonons
T = transverse mode

References

[1] Cahill, D. G., Ford, W. K., Goodson, K. E., Mahan, G. D., Majumdar, A., Maris, H. J., Merlin, R., and Phillpot, S. R., 2003, "Nanoscale Thermal Transport," J. Appl. Phys., **93**(2), pp. 793–818.
[2] Luo, T., and Chen, G., 2013, "Nanoscale Heat Transfer—From Computation to Experiment," Phys. Chem. Chem. Phys., **15**, pp. 3389–3412.
[3] Pop, E., 2010, "Energy Dissipation and Transport in Nanoscale Devices," Nano Res., **3**(3), pp. 147–169.
[4] Kapitza, P. L., 1941, "The Study of Heat Transfer in Helium II," J. Phys. USSR, **4**(181), pp. 1–31.
[5] Hopkins, P. E., 2013, "Thermal Transport Across Solid Interfaces With Nanoscale Imperfections: Effects of Roughness, Disorder, Dislocations, and Bonding on Thermal Boundary Conductance," ISRN Mech. Eng., **2013**, p. 682586.
[6] Wilson, R. B., and Cahill, D. G., 2012, "Experimental Validation of the Interfacial Form of the Wiedemann-Franz Law," Phys. Rev. Lett., **108**, p. 255901.
[7] Hopkins, P. E., Serrano, J. R., Phinney, L. M., Kearney, S. P., Grasser, T. W., and Harris, C. T., 2010, "Criteria for Cross-Plane Dominated Thermal Transport in Multilayer Thin Film Systems During Modulated Laser Heating," ASME J. Heat Transfer, **132**(8), p. 081302.
[8] Gundrum, B. C., Cahill, D. G., and Averback, R. S., 2005, "Thermal Conductance of Metal-Metal Interfaces," Phys. Rev. B, **72**, p. 245426.
[9] Clemens, B. M., Eesley, G. L., and Paddock, C. A., 1988, "Time-Resolved Thermal Transport in Compositionally Modulated Metal Films," Phys. Rev. B, **37**, pp. 1085–1096.
[10] Swartz, E. T., and Pohl, R. O., 1989, "Thermal Boundary Resistance," Rev. Mod. Phys., **61**, pp. 605–668.
[11] Norris, P. M., and Hopkins, P. E., 2009, "Examining Interfacial Diffuse Phonon Scattering Through Transient Thermoreflectance Measurements of Thermal Boundary Conductance," ASME J. Heat Transfer, **131**(4), p. 043207.
[12] Stoner, R. J., Maris, H. J., Anthony, T. R., and Banholzer, W. F., 1992, "Measurements of the Kapitza Conductance Between Diamond and Several Metals," Phys. Rev. Lett., **68**, pp. 1563–1566.
[13] Stoner, R. J., and Maris, H. J., 1993, "Kapitza Conductance and Heat Flow Between Solids at Temperatures From 50 to 300 K," Phys. Rev. B, **48**, pp. 16373–16387.
[14] Little, W. A., 1959, "The Transport of Heat Between Dissimilar Solids at Low Temperatures," Can. J. Phys., **37**(3), pp. 334–349.
[15] Huberman, M. L., and Overhauser, A. W., 1994, "Electronic Kapitza Conductance at a Diamond-Pb Interface," Phys. Rev. B, **50**, pp. 2865–2873.
[16] Sergeev, A. V., 1998, "Electronic Kapitza Conductance Due to Inelastic Electron-Boundary Scattering," Phys. Rev. B, **58**, pp. R10199–R10202.
[17] Sergeev, A., 1999, "Inelastic Electron-Boundary Scattering in Thin Films," Physica B, **263–264**, pp. 217–219.
[18] Grimvall, G., 1981, *Selected Topics in Solid State Physics*, North-Holland, New York.
[19] Mahan, G. D., 2009, "Kapitza Thermal Resistance Between a Metal and a Nonmetal," Phys. Rev. B, **79**, p. 075408.
[20] Lyeo, H.-K., and Cahill, D. G., 2006, "Thermal Conductance of Interfaces Between Highly Dissimilar Materials," Phys. Rev. B, **73**, p. 144301.
[21] Hopkins, P. E., 2009, "Effects of Electron-Boundary Scattering on Changes in Thermoreflectance in Thin Metal Films Undergoing Intraband Excitations," J. Appl. Phys., **105**(9), p. 093517.
[22] Hopkins, P. E., Duda, J. C., and Norris, P. M., 2011, "Anharmonic Phonon Interactions at Interfaces and Contributions to Thermal Boundary Conductance," ASME J. Heat Transfer, **133**(6), p. 062401.
[23] Duda, J. C., Norris, P. M., and Hopkins, P. E., 2011, "On the Linear Temperature Dependence of Phonon Thermal Boundary Conductance in the Classical Limit," ASME J. Heat Transfer, **133**(7), p. 074501.
[24] Singh, P., Seong, M., and Sinha, S., 2013, "Detailed Consideration of the Electron-Phonon Thermal Conductance at Metal-Dielectric Interfaces," Appl. Phys. Lett., **102**(18), p. 181906.
[25] Majumdar, A., and Reddy, P., 2004, "Role of Electron–Phonon Coupling in Thermal Conductance of Metal–Nonmetal Interfaces," Appl. Phys. Lett., **84**(23), pp. 4768–4770.
[26] Hopkins, P. E., and Norris, P. M., 2007, "Substrate Influence in Electron-Phonon Coupling Measurements in Thin Au Films," Appl. Surf. Sci., **253**(15), pp. 6289–6294.
[27] Hopkins, P. E., Kassebaum, J. L., and Norris, P. M., 2009, "Effects of Electron Scattering at Metal-Nonmetal Interfaces on Electron-Phonon Equilibration in Gold Films," J. Appl. Phys., **105**(2), p. 023710.
[28] Guo, L., Hodson, S. L., Fisher, T. S., and Xu, X., 2012, "Heat Transfer Across Metal-Dielectric Interfaces During Ultrafast-Laser Heating," ASME J. Heat Transfer, **134**(4), p. 042402.
[29] Ren, J., and Zhu, J.-X., 2013, "Heat Diode Effect and Negative Differential Thermal Conductance Across Nanoscale Metal-Dielectric Interfaces," Phys. Rev. B, **87**, p. 241412.
[30] Qiu, T. Q., and Tien, C. L., 1993, "Size Effects on Nonequilibrium Laser Heating of Metal Films," ASME J. Heat Transfer, **115**(4), pp. 842–847.
[31] Kaganov, M., Lifshitz, I., and Tanatarov, L. V., 1957, "Relaxation Between Electrons and the Crystalline Lattice," Sov. Phys. JETP, **4**(2), pp. 173–178.
[32] Anisimov, S. I., Kapeliovich, B. L., and Perelman, T. L., 1974, "Electron Emission From Metal Surfaces Exposed to Ultrashort Laser Pulses," Z. Eksp. Teor. Fiz., **66**, pp. 776–781.
[33] Hohlfeld, J., Wellershoff, S. S., Gudde, J., Conrad, U., Jahnke, V., and Matthias, E., 2000, "Electron and Lattice Dynamics Following Optical Excitation of Metals," Chem. Phys., **251**(1–3), pp. 237–258.
[34] Lin, Z., Zhigilei, L. V., and Celli, V., 2008, "Electron-Phonon Coupling and Electron Heat Capacity of Metals Under Conditions of Strong Electron-Phonon Nonequilibrium," Phys. Rev. B, **77**, p. 075133.
[35] Mueller, B. Y., and Rethfeld, B., 2013, "Relaxation Dynamics in Laser-Excited Metals Under Nonequilibrium Conditions," Phys. Rev. B, **87**, p. 035139.
[36] Fann, W. S., Storz, R., Tom, H. W. K., and Bokor, J., 1992, "Electron Thermalization in Gold," Phys. Rev. B, **46**, pp. 13592–13595.
[37] Weber, W., 1977, "Adiabatic Bond Charge Model for the Phonons in Diamond, Si, Ge, and α—Sn," Phys. Rev. B, **15**, pp. 4789–4803.
[38] Hopkins, P. E., Beechem, T. E., Duda, J. C., Smoyer, J. L., and Norris, P. M., 2010, "Effects of Subconduction Band Excitations on Thermal Conductance at Metal-Metal Interfaces," Appl. Phys. Lett., **96**(1), p. 011907.
[39] Duda, J. C., Beechem, T. E., Smoyer, J. L., Norris, P. M., and Hopkins, P. E., 2010, "Role of Dispersion on Phononic Thermal Boundary Conductance," J. Appl. Phys., **108**(7), p. 073515.
[40] Duda, J. C., Hopkins, P. E., Smoyer, J. L., Bauer, M. L., English, T. S., Saltonstall, C. B., and Norris, P. M., 2010, "On the Assumption of Detailed Balance in Prediction of Diffusive Transmission Probability During Interfacial Transport," Nanoscale Microscale Thermophys. Eng., **14**(1), pp. 21–33.
[41] Sellan, D. P., Turney, J. E., McGaughey, A. J. H., and Amon, C. H., 2010, "Cross-Plane Phonon Transport in Thin Films," J. Appl. Phys., **108**(11), p. 113524.
[42] Duda, J. C., Yang, C.-Y. P., Foley, B. M., Cheaito, R., Medlin, D. L., Jones, R. E., and Hopkins, P. E., 2013, "Influence of Interfacial Properties on Thermal Transport at Gold: Silicon Contacts," Appl. Phys. Lett., **102**(8), p. 081902.
[43] Hopkins, P. E., Duda, J. C., Kaehr, B., Wang Zhou, X., Peter Yang, C.-Y., and Jones, R. E., 2013, "Ultrafast and Steady-State Laser Heating Effects on Electron Relaxation and Phonon Coupling Mechanisms in Thin Gold Films," Appl. Phys. Lett., **103**(21), p. 211910.